Dual-Objective Accelerated Linear Convergence Spotted Hyena Optimization for Power Enhancement in Partially Shaded PV Arrays

Swetha K.T. and B. Venugopal REDDY

***Abstract*—Partial shading (PS) presents a significant concern in PV arrays due to its substantial impact on system performance, causing reduced power output, distorted PV characteristics, and power loss. Therefore, this paper introduces a novel accelerated linear convergence factor-based spotted hyena optimization for dynamic PV array reconfiguration (DPVAR). The key aim of the accelerated linear convergence factor is to reduce row difference in each tier while minimizing the need to relocate modules, within a significantly reduced iteration count. The algorithm pursues two primary objectives: enhancing power generation under PS and efficiently finding the global maximum power within a minimum period while minimizing steady-state oscillations. Furthermore, the proposed algorithm is adaptable to dynamic PS conditions and applicable for symmetric and asymmetric PV arrays of any size. The effectiveness of the technique is evaluated through simulation and experiments. In addition, the performance of the proposed technique is compared to the particle swarm optimization (PSO) based reconfiguration method. The investigation reveals that the proposed reconfiguration technique demonstrates an average power enhancement of 17.57% compared to the before-reconfiguration method and 7.88% compared to the PSO reconfiguration method.**

***Index Terms*—Irradiance equalization, metaheuristic algorithm, power enhancement, partial shading condition, PV array reconfiguration, spotted hyena optimization.**

I. Introduction

PHOTOVOLTAIC (PV), energy generation has emerged as the most favored and preferred source of energy, playing a significant role in advancing the global energy scenario [1]. However, PV system encounters a significant challenge, namely, operating under non-uniform irradiance, which greatly affects power generation, P-V (power-voltage) characteristics, and overall reliability [2], [3]. Non-uniform irradiance, caused by shadows in partial shading conditions (PSC), is a major concern that leads to multiple peaks in the PV curve [4]. Consequently, the PV array experiences a significant difference in current between rows within the PV array [5]. To address these issues, array reconfiguration techniques like static and dynamic have been proposed as a solution to mitigate the impact of shading [6]. The static reconfiguration process involves physical relocation of PV modules within the array to disperse shade [7]. Different static reconfiguration techniques such as sudoku [8], arithmetic sequence pattern reconfiguration technique [9], magic square view [10], novel shade dispersion technique [11] etc. have been proposed in literature to relocate the PV modules. However, these physical relocation methods have inherent drawbacks [12], including labour requirement, lengthy cables, dependence on sub-arrays, need for arbitrary assumptions during implementation and incompatibility with asymmetrical PV arrays.

The electrical array reconfiguration (EAR) is a dynamic process that employs simultaneous switching patterns to reconfigure the interconnections of a PV array, aiming to achieve row equalization based on shade patterns [13]. As a result, EAR represents a promising solution when compared to conventional PV array reconfiguration (PVAR) approaches. Numerous research studies have utilized EAR for power enhancement in PV arrays [14]. However, achieving the desired switching patterns for shade dispersion in the EAR method is often accomplished using a trial-and-error approach, which may not be highly efficient [15]. Consequently, the processing time required to achieve the optimal switching matrix increases. Furthermore, the frequent switching involved in the reconfiguration process can have a negative impact on the lifespan of relay. To overcome the aforementioned drawback, optimization algorithms are used as an alternative solution, such as, the butterfly optimization algorithm [16], artificial ecosystem-based optimization [17], improved equilibrium optimization [18] and particle swarm optimization (PSO) [19], have been recently employed for shade dispersion in the PV array. Optimization methods based on dynamic PVAR offer several advantages including: 1) They are designed to efficiently converge towards optimal solutions, thereby reducing the time required to achieve the desired outcome. 2) Aim to minimize the difference in current among rows in the PV array. However, the existing algorithms involve complex mathematical calculations, sensitive to tuning parameters, it involves multiple iterations in the evaluation of fitness functions, which can lead to a computational burden on the system, algorithms can converge to local minima instead of the

Manuscript received November 26, 2023; revised February 24, 2024, June 23, 2024; accepted August 12, 2024. Date of publication September 30, 2024; date of current version August 30, 2024. No funding was received to assist with the preparation of this manuscript. *(Corresponding author: Swetha K.T.)*

All authors are with the Department of Electrical and Electronics Engineering from the National Institute of Technology Goa, Ponda, India (e-mail: swethakt.nitg@gmail.com; bvenugopalreddy@nitgoa.ac.in).

Digital Object Identifier 10.24295/CPSSTPEA.2024.00016

global optimum, and they are sensitivity to initial conditions.

In this paper, an accelerated linear convergence spotted hyena optimization (ALC-SHO) based dynamic PVAR technique is proposed, with the enhanced capability of shade dispersion. The proposed ALC-SHO algorithm accomplishes two objectives: it reconfigures the PV modules into their optimal positions to achieve irradiance equalization as the first objective, and simultaneously, it maximizes power extraction by tracking global maximum power point (GMPP) while minimizing the steady-state oscillations and tracking time under PSCs, as the second objective. The accelerated linear convergence factor is implemented to achieve the minimum row current difference with fewer module relocations. Consequently, this approach reduces the required number of switch activations. In addition, by employing a single tuning parameter, the complexity associated with finetuning multiple parameters is effectively circumvented. The performance of the proposed algorithm is more effective than the conventional SHO (CSHO) algorithm. The proposed algorithm is implemented on a 3×3 PV array and compared with before-reconfiguration, and after-reconfiguration methods using PSO [19], and CSHO [20]. The proposed method is simulated using Matlab. Further, the proposed algorithm is verified using an experimental prototype under various PSCs. The comparison is based on several factors, including power enhancements, mismatch losses, percentage power loss, and irradiance equalization (IE) under different PSCs.

The main contributions of this paper are as follows:

1) The first contribution is proposed on ALC-SHO-based reconfiguration to re-arrange the PV modules to achieve IE between each rows, thereby enhancing the power.
2) The second contribution is the extraction of enhanced power using the proposed ALC-SHO-based maximum power point tracking (MPPT) algorithm, which ensures fast convergence with negligible steady-state error.
3) An experimental study is performed on the proposed method and compared with the conventional methods.
4) Comparative analysis is performed to show the effectiveness of the proposed system in terms of mismatch power loss, and percentage of power loss.

The rest of the paper is structured as follows: Section II presents the introduction to the novel ALC-SHO algorithm and is followed by implementation steps for PVAR and MPPT in Section III. In Section IV, the simulation result and discussion for the proposed dynamic PVAR method under various shading conditions are summarized. Section V presents the experimental results. Finally, Section VI summarises and concludes the key findings.

II. Accelerated Linear Convergence Spotted Hyena Optimization

The spotted hyena optimization (SHO) [21], draws inspiration from the social behavior and hunting strategies of spotted hyenas. Spotted hyenas engage in four key operations: search, encirclement, hunting, and attacking their prey. This section presents the mathematical models for each of these processes.

1) Encircling: Assuming that the target prey represents the current best solution, the remaining search agents will adjust their positions toward this best solution. The mathematical model for the encircling process can be described as follows:

$$D_{\mathrm{h}} = | B \times X_{\mathrm{P}}(t) - X(t) | \tag{1}$$

$$X(t+1) = | X_{\mathrm{P}}(t) - E \times D_{\mathrm{h}} | \tag{2}$$

where B and E denote the coefficients, X_{P} is the position of prey, X indicates the position of hyenas, D_{h} represents the distance between the prey and the spotted hyena, and t denotes the current iteration. The coefficient vectors B and E are given in (3) and (4) respectively.

$$B = 2 \times r_1 \tag{3}$$

$$E = 2 \times a \times r_2 - a \tag{4}$$

$$a = 5 - \frac{itr \times 5}{itr_{\max}} \tag{5}$$

where r_1, and r_2 are random variables in the range [0, 1], itr is denoted as the iteration number, $itr_{\max}$ is the maximum iteration required, and a is a convergence factor that falls linearly from 5 to 0.

This paper proposes an accelerated linear convergence factor (a_{alc}), which plays a significant role in finding an optimum point. It is essential to coordinate with exploration and exploitation to determine the optimum solution.

$$a_{\mathrm{alc}} = \frac{1}{n^2}\left(\frac{itr_{\max} - itr}{itr_{\max}}\right) \tag{6}$$

where, 'n' is the accelerated convergence parameter ranging between [0, 4]. The key role of 'n' is to navigate and converge towards an optimal solution with less number of iterations. When 'n' is set to lower values, exploration takes place. The algorithm aims to discover new possibilities by stepping into unknown areas of the solution space. When 'n' is set to higher values (closer to 4), the algorithm exploits and tries to refine its search around promising solutions to find the best possible solution. The impact of 'n' parameter on algorithm behavior is shown in Fig. 1 and demonstrates the transition from exploration to exploitation as 'n' increases. It plays a crucial role in optimizing the convergence speed of the algorithm. The larger the value of a, the stronger the global search capability. Thus, hyenas avoid settling into a local optimum. A smaller value of a indicates better exploitation, which speeds up the convergence. However, in the existing SHO method, the convergence factor a decreases linearly from 5 to 0 as the number of iterations increases, as given in (5). Further, the linearly decreasing approach of the convergence factor a has an good global search ability, but the convergence rate is slow. Hence, in this paper, an accelerated linear convergence factor a_{alc} is proposed, which decreases linearly from 1 to 0, as given in (6). Therefore, the accelerated linearly decreasing quantity is better than the linearly decreasing quantity, thereby showing better global search ability with a rapid convergence rate and reduced iteration count as depicted in Fig. 1(b). The outcomes

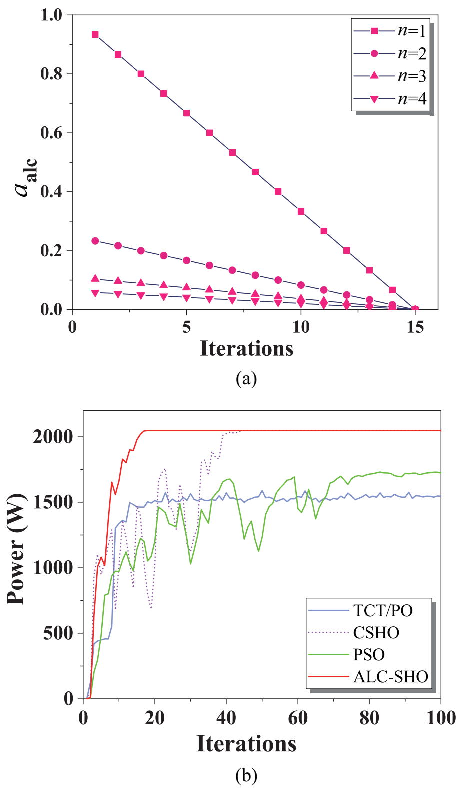

Fig. 1. (a) Impact of parameter ‘n’ on algorithm behavior. (b) Relation between iteration and power.

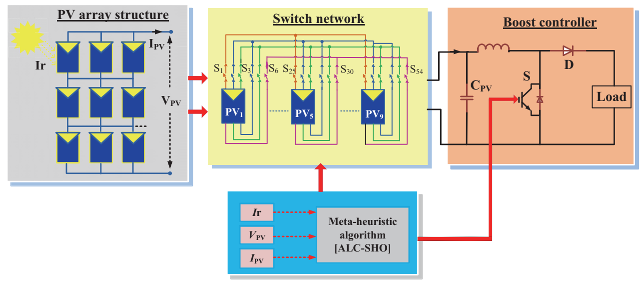

Fig. 2. Block diagram of the ALC-SHO based solar PV reconfiguration for a stand-alone system.

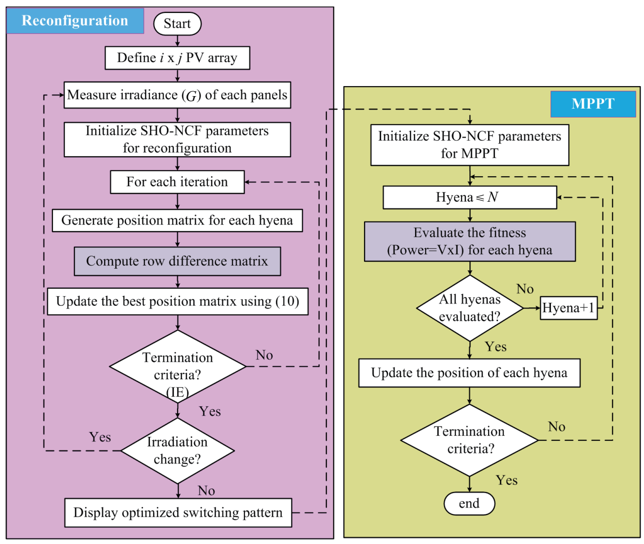

Fig. 3. Flowchart for ALC-SHO based PVAR.

of the modified convergence factor a_{alc} is better than those of the existing CSHO algorithm.

2) Hunting: The spotted hyenas hunt in packs and have the ability to locate the prey. The hunting mechanism is determined using (7) and (8). The other search agents form a cluster (C_{h}) towards the best search agent and save the best solutions in each iteration to update their positions.

$$D_{\mathrm{h}} = |\, B \times X_{\mathrm{h}}(t) - X(k) \,| \tag{7}$$

$$X_k = X_{\mathrm{h}} - E \times D_{\mathrm{h}} \tag{8}$$

$$C_{\mathrm{h}} = [\, X_k, X_{k+1}, \ldots, X_{k+N} \,] \tag{9}$$

3) Attacking: It is feasible to assault the prey mathematically by decreasing the a_{alc} value. The variation in E is also responsible for changing the value of a_{alc}.

4) Search for prey: According to the cluster (C_{h}), the spotted hyenas search for prey. They move farther apart to hunt and assault the prey. The coefficients B and E are used to explore and avoid local optima.

III. ALC-SHO Implementation to PVAR

A. Optimization Problem Definition

The optimization technique plays an important role in the rearrangement of panels, leading to enhanced power generation. While traditional dynamic PVAR methods increase the output power, they often fail to identify the best configuration [22]. However, this limitation is addressed by the proposed ALC-SHO algorithm. The ALC-SHO algorithm ensures the determination of the optimal configuration through its four operations. This optimization technique follows a sequence of steps to locate the optimal solution. The block diagram of the proposed system is depicted in Fig. 2. The procedure of the proposed method for solving the reconfiguration process is illustrated in the flowchart shown in Fig. 3. When shading occurs, the irradiance on individual PV panels is estimated and forms a generalized PV irradiance matrix. Subsequently, the proposed ALC-SHO algorithm is initiated to alleviate the levels of mismatch by minimizing the difference in row currents. Once the optimal solution is obtained, a switching matrix is identified, aligning with the reconfigured irradiance values. Finally, the PV panels that have undergone reconfiguration are linked to either stand-alone system, where the proposed ALC -SHO algorithm tracks GMPP. The ALC-SHO algorithm is employed to achieve the following objectives: 1) Minimize the irradiance difference among the rows of PV array and reduce multiple peaks in the P-V curve. 2) Determine the optimal switching combination from multiple possibilities, resulting in effective shade dispersion. 3) Track the actual GMPP with minimal steady-state oscillations. 4) Minimize the tracking period.

B. The Implementation Steps for PVAR

1) Initialization for reconfiguration matrix: The size of PV array is represented as $i \times j$, where i represents the number of rows and j represents the number of columns.
2) Evaluation of the hyena matrix: The objective function is to achieve IE. By minimizing the difference in irradiance among the rows, a uniform distribution of shade across the PV array can be achieved. This shading pattern aims to maximize the output power of the PV system by reducing variations and errors in row irradiance.

$$Ir_i = \sum_j Ir_{ij} \tag{10}$$

$$Ir_{\max} = \max\,(Ir_1, Ir_2, ..., Ir_i) \tag{11}$$

$$Ir_{\mathrm{err}} = \sum_i (Ir_{\max} - Ir_i) \tag{12}$$

where Ir_{ij} represents the irradiance of the $i \times j$ module, Ir_{err} denotes the sum of the error difference between maximum row irradiance ($Ir_{\max}$) and ith row irradiance of the PV array (Ir_i).

3) Updating the matrix: In this step, the ALC-SHO algorithm is utilized to identify the optimal switching matrix that minimizes the difference in row irradiance and maximizes the power output of the PV array. This is accomplished by evaluating the irradiation level of each row and comparing it with the previous iterations and updating using four operations of the proposed algorithm. The algorithm continues the procedure until the optimal switching performance is achieved. If any changes in irradiance are detected, the proposed algorithm will automatically reinitialize for IE.
4) Termination criteria: Once the minimum irradiance difference between each row is reached, the algorithm concludes its search and updating process for the matrix elements. The objective of minimizing the row-to-row irradiance difference has been achieved at this point.
5) Change in irradiance: After reaching the termination criteria, if any changes in irradiance are detected, the hyenas undergo a re-initialization process to search for a new solution.
6) Switching matrix: The switching matrix represents the switching actions required to implement the reconfigured PV array obtained from the ALC-SHO algorithm. When the termination criteria is met, the proposed algorithm transmits the necessary switching instructions to initiate the newly optimized reconfigured PV array. The total number of single pole double throw (SPDT) switches required for symmetric (i×i) size of PV array (2×2, 3×3, etc.) is calculated using (13),

$$2 \times i^2 \times (i-1) \quad \text{where, } i = j. \tag{13}$$

The required SPDT switch for asymmetric PV array structure (i×j) (3×4, 4×5 etc.) is given in (14),

$$2 \times i^2 \times (i^2 - 1) \quad \text{where, } i < j. \tag{14}$$

C. The Implementation Steps for ALC-SHO-Based MPPT

1) Initialization: In the ALC-SHO based MPPT, the position of each hyena corresponds to the duty ratio of the boost converter. The hyenas are initially scattered randomly within the search space, taking into account the duty ratio constraints of $D_{\max} = 0.8$ and $D_{\min} = 0.2$.
2) Fitness evaluation: The main objective is to maximize the power extracted from the PV array by appropriately adjusting the duty ratio of the boost converter. The algorithm aims to operate the converter at the point that results in the maximum power output from the PV array.

$$\text{Maximize } P = f(D) \quad \text{subject to } D_{\min} \leqslant D \leqslant D_{\max} \tag{15}$$

3) Position update: The positions of the hyenas are updated based on a comparison between the power values of the previous iteration $P[D(t)]$ and the present iteration $P[D(t+1)]$. If the power obtained from the present iteration is greater ($P[D(t+1)] > P[D(t)]$), then the positions of hyenas are updated. However, if the power remains same or decreases, the positions of the hyenas are retained without any changes. This process ensures that the hyenas move towards positions that lead to higher power output from the array while avoiding the moves that would lead to a reduction in power.
4) Avoid repeated exploration: The proposed accelerated linear convergence factor a_{alc} is designed to decrease gradually from 1 to 0 during the course of the iteration. The algorithm can quickly converge to the optimal solution, enabling efficient and swift determination of the GMPP, by gradually reducing the convergence factor.
5) Termination criteria: The termination criteria is satisfied when both the ΔP (change in power) and ΔD (change in duty ratio) are less than 5%. This criterion indicates that all the hyenas have converged to the maximum power point (MPP) within the specified tolerance. Once these conditions are met, the algorithm terminates.

IV. Simulation Results and Discussion

The performance of ALC-SHO-based PVAR is evaluated for three different sizes of PV array. In the initial case, a 3×3 PV array is subjected to two different shading patterns. The objective is to assess the ability of ALC-SHO algorithm to disperse shade effectively in a PV array and analyze its effectiveness in maximizing power output. In the second case, two asymmetric 3×4 PVAR is evaluated, further demonstrating the adaptability of the algorithm in addressing the complex PVAR. The proposed ALC-SHO algorithm-based PVAR is applied for a larger size (6×6) PV array lastly. This case aims to verify the performance of the algorithm on a larger-size PV array. The specifications of the PV module is as follows: Open circuit voltage (V_{oc}) is 44.4 V, short circuit current (I_{sc}) is 8.6 A, the voltage at MPP (V_{mpp}) is 36.6 V, current at MPP (I_{mpp}) is 8.2 A and the power at MPP (P_{mpp}) is 300.12 W. Four different shading patterns are considered to verify the effectiveness of the proposed ALC-SHO algorithm.

1) PSC-1: Column shade pattern.
2) PSC-2: Triangular shade pattern.

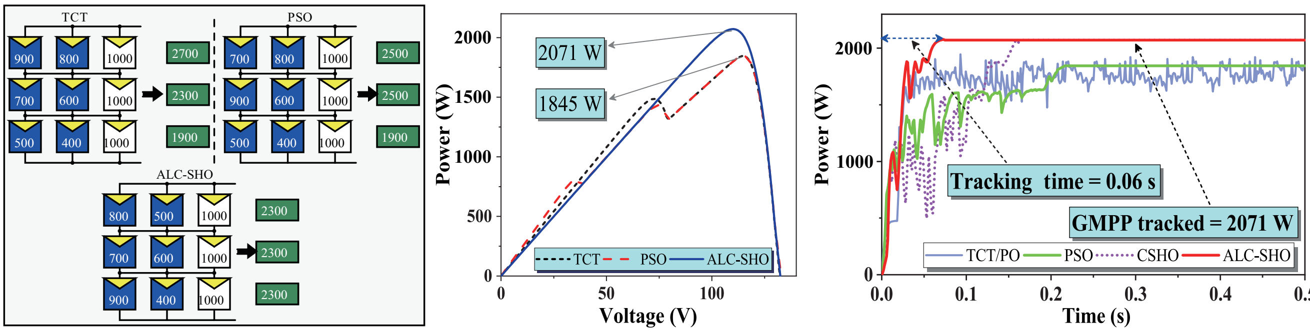

(a) (b) (c)

Fig. 4. The simulation results for column shading pattern. (a) PV panel arrangement, (b) P-V characteristics and (c) GMPP tracking.

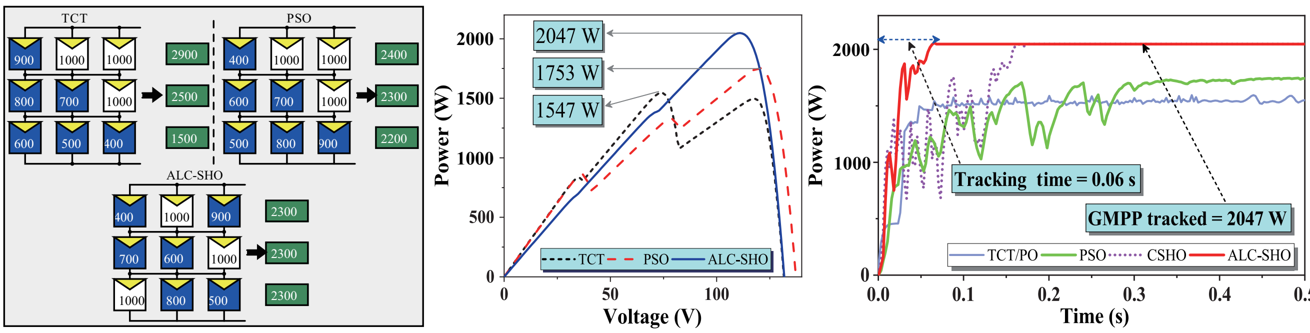

(a) (b) (c)

Fig. 5. The simulation results for triangular shading pattern. (a) PV panel arrangement, (b) P-V characteristics and (c) GMPP tracking.

3) PSC-3: Corner shade pattern.
4) PSC-4: L-shape shade pattern.

A. Performance Analysis of ALC-SHO for 3×3 PVAR(Symmetric)

In this subsection, the simulation results of the proposed ALC-SHO$_{(\text{Reconfiguration/MPPT})}$ (ALC-SHO$_{R/M}$) algorithm is presented for a 3×3 PV array using the switch network under various PSCs. The performance of the algorithm is compared with TCT$_{\text{Configuration}}$/PO$_M$, CSHO$_{R/M}$, and PSO$_{R/M}$.

1) PSC-1/Column shade pattern: The proposed algorithm aims to rearrange the PV modules until the minimum difference in row irradiance is achieved, as shown in Fig. 4(a). This reconfiguration process results in a uniform P-V curve, as evident from Fig. 4(b). The proposed algorithm successfully tracks an enhanced PV power of 2071 W within 0.06 s, whereas the CSHO algorithm tracks maximum power of 2071 W in 0.165 s as shown in Fig. 4(c). Though the power enhanced after reconfiguration by both the algorithms are same, the proposed ALC-SHO algorithm takes less time for tracking GMPP compared to CSHO. In contrast, before reconfiguration using TCT$_C$ /PO$_M$ extracts maximum power of 1795 W as tabulated in Table I. It is worth noting that steady-state oscillation occurs around the MPP, resulting in power loss. Further, PSO$_{R/M}$ algorithm achieves 1845 W and the required tracking time is 0.16 s. Therefore, the proposed ALC-SHO$_{R/M}$ method enhances the output power by 13.2% and 10.91% compared to before-reconfiguration (TCT$_C$ /PO$_{MPPT}$) and after-reconfiguration (PSO$_{R/M}$), respectively.

TABLE I
COMPARATIVE ANALYSIS OF SIMULATION RESULTS

PSCs	TCT$_C$ /PO$_M$		PSO$_{R/M}$		CSHO$_{R/M}$		ALC-SHO$_{R/M}$	
	Power/ W	Time/ s	Power/ W	Time/ s	Power/ W	Time/ s	Power/ W	Time/ s
PSC-1	1795	0.03	1845	0.16	2071	0.165	2071	0.06
PSC-2	1503	0.03	1753	0.15	2047	0.155	2047	0.06
PSC-3	2459	0.06	2915	0.14	2973	0.11	2973	0.054
PSC-4	2562	0.03	3022	0.19	3089	0.1	3089	0.06

2) PSC-2/Triangular shade pattern: The proposed reconfiguration algorithm is able to achieve a uniform PV curve, as shown in Fig. 5(b). The proposed algorithm effectively tracks an improved PV power of 2047 W within 0.06 s, whereas CSHO method tracks maximum power of 2047 W in 0.155 s as depicted in Fig. 5(c). In comparison, before-reconfiguration TCT$_C$ /PO$_M$ method extracts a maximum power 1503 W and in addition, it exhibits steady-state oscillation, resulting in power loss within the system. The PSO$_{R/M}$ algorithm tracks power to 1753 W and the time required to track the maximum power is 0.36 s. Therefore, the proposed ALC-SHO$_{R/M}$ method enhances the output power by 26.57% and 14.36%, compared to before-reconfiguration using TCT$_C$ /PO$_M$ and after reconfiguration using the PSO$_{R/M}$ method, respectively.

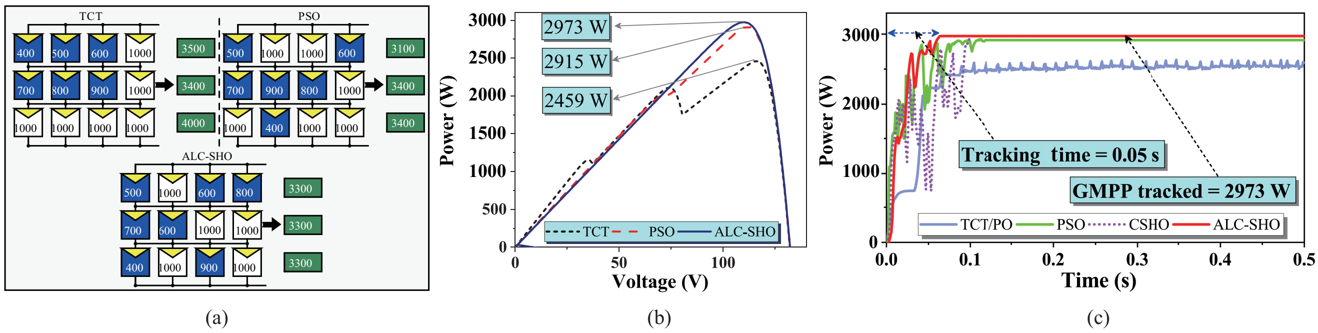

Fig. 6. The simulation results for corner shading pattern. (a) PV panel arrangement, (b) P-V characteristics and (c) GMPP tracking.

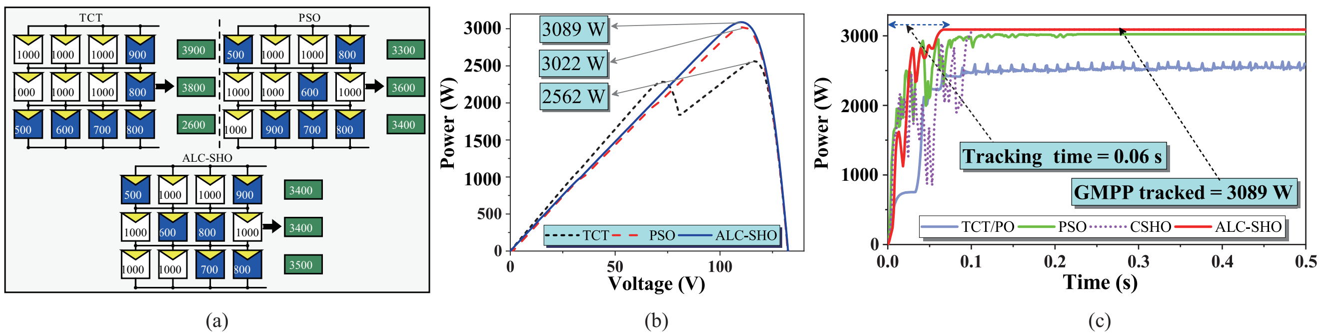

Fig. 7. The simulation results for asymmetric shading pattern. (a) PV panel arrangement, (b) P-V characteristics and (c) GMPP tracking.

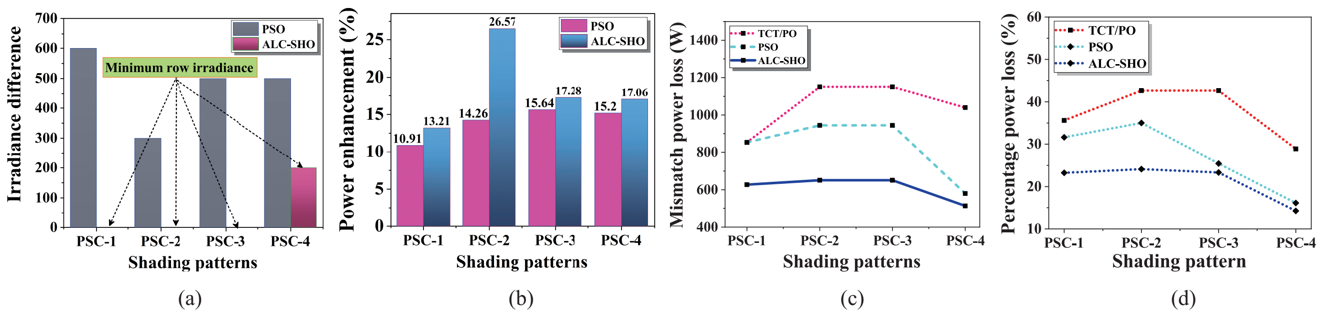

Fig. 8. (a) Row irradiance difference. (b) Power enhancement w.r.t before-reconfiguration. (c) Mismatch power loss. (d) Percentage power loss.

B. Performance Analysis of ALC-SHO for 3×4 PVAR (Asymmetric)

1) PSC-3/Corner shade pattern: The implementation of the proposed reconfiguration process leads to a uniform PV curve, as observed in Fig. 6(b). The proposed algorithm significantly improves the power output of 2973 W with a tracking time of 0.054 s, while CSHO algorithm improves power of 2973 W and tracks GMPP within 0.11 s, as illustrated in Fig. 6(c). It can be observed that the proposed and the conventional algorithms effectively track maximum power. However, the conventional method takes longer to track the GMPP. In comparison, the TCT_C /PO_M method extracts a maximum power of 2459 W. However, it is accompanied by steady-state oscillation, leading to power loss within the system. On the other hand, the $PSO_{R/M}$ algorithm tracks the maximum power of 2915 W, and it requires a longer tracking time of 0.14 s. As a result, the proposed $ALC\text{-}SHO_{R/M}$ technique outperforms TCT_C /PO_M and $PSO_{R/M}$ techniques by increasing the output power by 8.24% and 5.79%, respectively.

2) PSC-4/L-shape shade pattern: The proposed and CSHO algorithm effectively improves the power of 3089 W and the time required to track the improved PV output power is 0.06 s and 0.1 s, respectively, and is depicted in Fig. 7(c). In comparison, the TCT_C /PO_M algorithm extracts a maximum power of 2562 W. Furthermore, the PSO algorithm enhances the output power of 3022 W, and it requires a longer tracking time of 0.2 s. Consequently, the proposed $ALC\text{-}SHO_{R/M}$ technique outperforms TCT_C /PO_M and $PSO_{R/M}$ techniques by increasing the power by 17.06% and 2.16%, respectively.

C. Performance Analysis of the Proposed Algorithm

Fig. 8 illustrates the performance analysis of the proposed and conventional algorithms. Fig. 8(a) depicts the row irradiance difference of each algorithm, it is inferred that the proposed algorithm has less irradiance difference between each row.

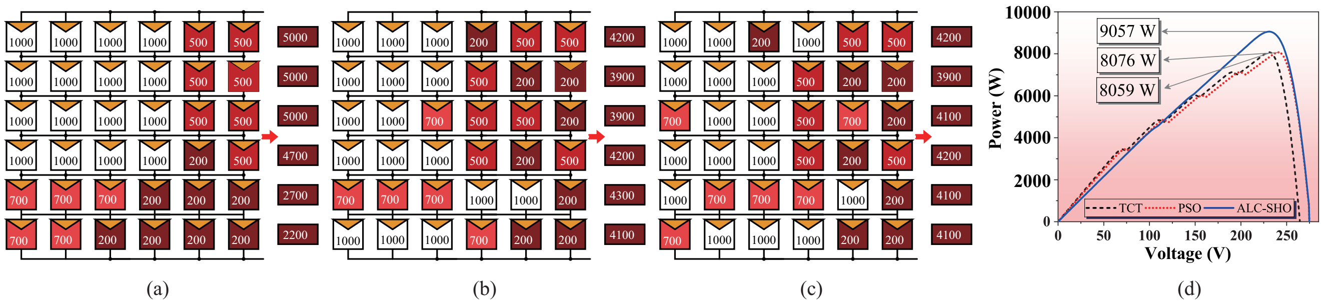

Fig. 9. Shade dispersion under long-narrow shading pattern considering. (a) TCT, (b) PSO, (c) ACL-SHO and (d) P-V characteristics.

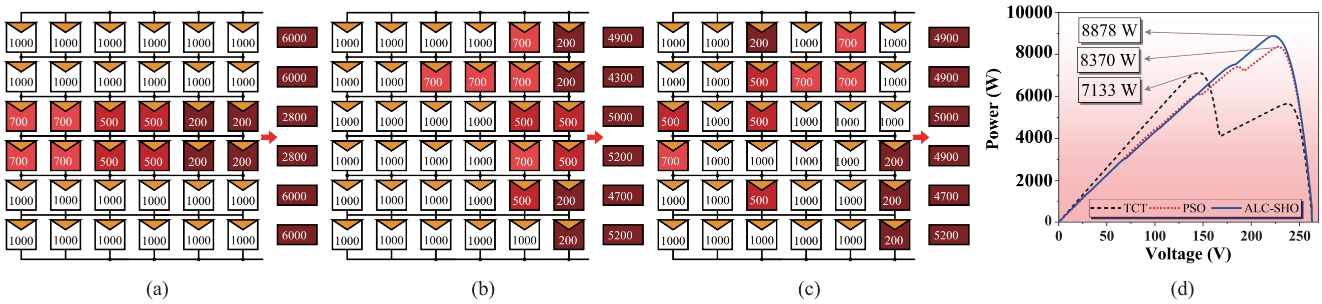

Fig. 10. Shade dispersion under horizontal shading pattern considering. (a) TCT, (b) PSO, (c) ACL-SHO and (d) P-V characteristics.

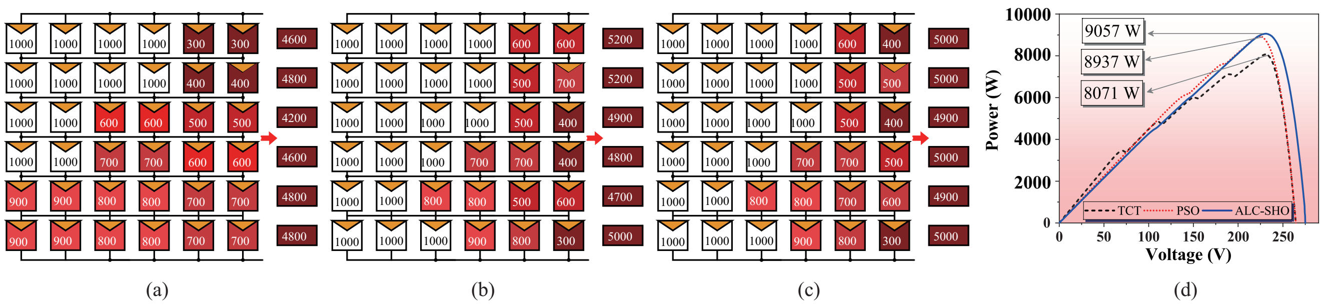

Fig. 11. Shade dispersion under step shading pattern considering. (a) TCT, (b) PSO, (c) ACL-SHO and (d) P-V characteristics.

The proposed algorithm demonstrates an average power enhancement of 17.57% compared to before-reconfiguration and a 7.88% power enhancement compared to the $PSO_{R/M}$ method as shown in Fig. 8(b). Further, the mismatch and percentage power loss of the proposed algorithm are lower as depicted in Fig. 8(c) and (d).

D. Performance Analysis of ALC-SHO for m×n PV Array

The proposed algorithm has successfully reconfigured 3×3 PV array using $ALC\text{-}SHO_{R/M}$ algorithm. However, this algorithm can be extended to PV array of any size. In this section, 6×6 PV array is considered and in addition, it is compared with $PSO_{R/M}$ algorithm. The shade dispersion and the P-V characteristics of each algorithm is shown in Figs. 9–11. It can be inferred from the P-V graphs that the proposed reconfiguration technique outperforms in dispersing the shade pattern and achieving maximum power.

V. Experimental Results

The proposed $ALC\text{-}SHO_{R/M}$ algorithm-based PV system is depicted in Fig. 12. The PV array characteristics are emulated using the solar array simulator. Additionally, the Opal-RT 4500 is employed to generate PWM signals for the DC-DC converter. The voltage and current sensors used in the setup are the LV-20p and LA-25p, respectively. A mixed signal oscilloscope (MSO46) records system responses. The PV system specification is as follows: V_{oc} = 80 V, V_{mp} = 65 V, I_{mp} = 2.43 A, I_{sc} = 2 A, P_{mp} = 150 W. The followings are the specifications of DC-DC boost converter, C_{in} = 100 µF, C_{out} = 250 µF, L = 2 mH, f_s = 10 kHz. Two shading conditions are considered, to experimentally validate the performance of the proposed algorithm. Furthermore, the proposed algorithm is compared with the TCT_C /PO_M, $PSO_{R/M}$ and $CSHO_{R/M}$ algorithms. The total number of particles used for reconfiguring the PV modules by the algorithms is 12. Increasing the number of particles in the algorithm typically leads to a larger

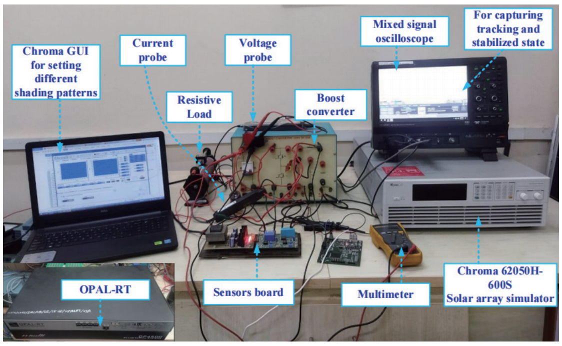

Fig. 12. Experimental prototype of the ALC-SHO based DPVAR method.

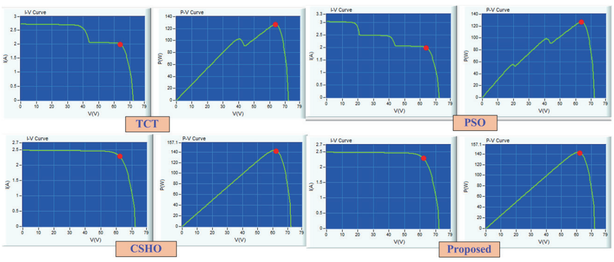

(a)

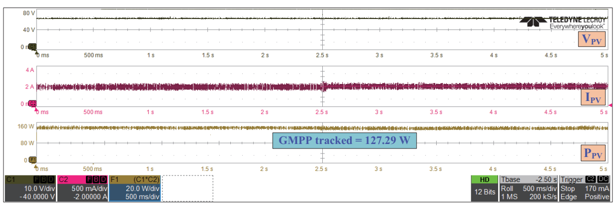

(b)

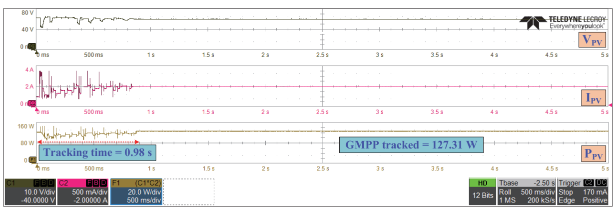

(c)

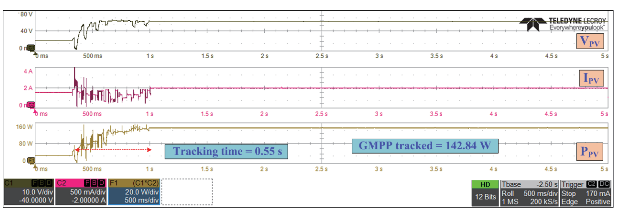

(d)

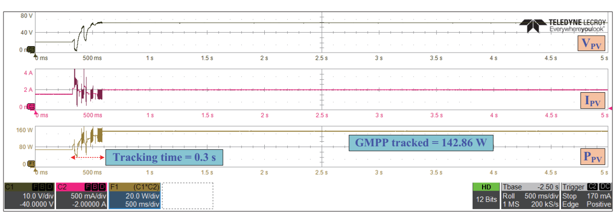

(e)

Fig. 13. The experimental results for 3×3 PV array under PSC-1 (Column shade pattern). (a) I-V and P-V curves. (b) TCT_C /PO_M. (c) $PSO_{R/M}$. (d) $CSHO_{R/M}$. (e) ALC-$SHO_{R/M}$.

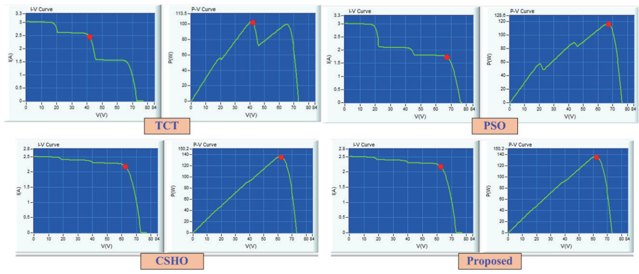

(a)

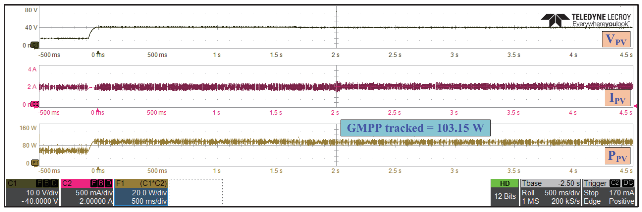

(b)

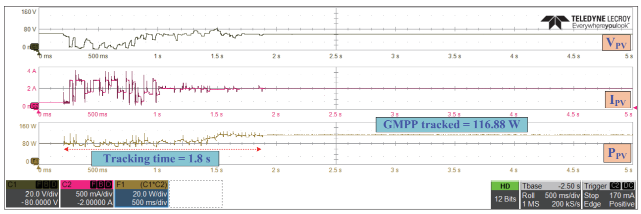

(c)

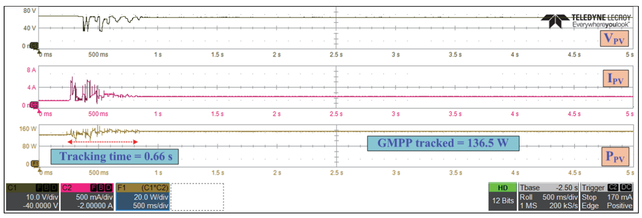

(d)

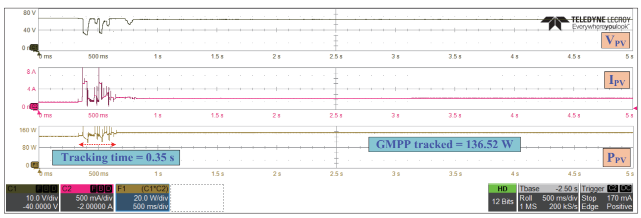

(e)

Fig. 14. The experimental results for 3×3 PV array under PSC-2 (Triangular shade pattern). (a) I-V and P-V curves. (b) TCT_C /PO_M. (c) $PSO_{R/M}$. (d) $CSHO_{R/M}$. (e) ALC-$SHO_{R/M}$.

exploration of the search space. However, it's important to note that this expanded exploration leads to increased computational time. With more particles, the algorithm requires additional iterations to converge towards GMPP. Moreover, ALC-SHO is able to balance between exploration and exploitation with a fewer number of particles. Indeed, in the pursuit of the global optimum, PSO algorithm often employs a larger number of particles. Thus, while more exploration is beneficial, the longer computational time can be considered a drawback. Furthermore, with fewer particles, there is a higher chance of being trapped in a local optimum solution.

1) The performance of the ALC-SHO algorithm is investigated under PSC-1: The P-V and I-V characteristics of TCT_C/PO_M, $PSO_{R/M}$, $CSHO_{R/M}$ and proposed methods for symmetric 3×3 under the column shading pattern is shown in Fig. 13(a). In this shading pattern, the TCT_C /PO_M method demonstrates a notable decrease in output power, tracking 127.29 W. Additionally, steady-state oscillations are also found around the MPP as shown in Fig. 13(b). The $PSO_{R/M}$ method failed to effectively disperse the shade across the PV array. The power output achieved by the TCT_C /PO_M and $PSO_{R/M}$ methods are the same. This is due to the performance of PSO which depends on its parameters, such as the inertia weight, cognitive, and social components. Proper tuning of these parameters can help the algorithm to explore the search space effectively while preventing premature convergence to local power point, however, tuning of these parameters is complex and time consuming. Furthermore, the $PSO_{R/M}$ algorithm requires a longer duration of 0.98 s to track the GMPP. The CSHO algorithm is enhances the power to 142.85 W and tracks GMPP in 0.55 s. The proposed algorithm improves the power of 142.86 W and is able to track within 0.3 s with negligible steady-state oscillations. Therefore, the ALC-SHO exhibits a lower number of peaks and a significant power enhancement of 10.89% compared to the existing configurations.

2) The performance of the ALC-SHO algorithm is investigated under PSC-2: Here, 3×3 symmetric shading conditionis considered. The TCT_C /PO_M method achieves 103.15 W. Moreover, significant steady-state oscillations are observed around the MPP, as shown in Fig. 14(a). The $PSO_{R/M}$ method enhances the power output by 116.86 W. It is worth noting that the $PSO_{R/M}$ algorithm requires a longer duration of 1.8 s, to track GMPP. Inefficient initialization or parameter settings can prolong the convergence process, as the PSO may struggle to effectively explore the search space and adjust particle trajectories towards the GMPP. Further, due to repeated exploration of the particle also leads to longer convergence period. The CSHO improves the power of 136.5 W and tracks GMPP in 0.66 s. The ALC-SHO not only enhances power output by 136.52 W, but it has ability to track within a 0.35 s, minimizing the steady-state oscillations as shown in Fig. 14(d).

VI. Conclusions

The paper presents a novel ALC-SHO algorithm for the optimal reconfiguration of a partially shaded PV array. The primary objective of the proposed method is to enhance the power from the PV array under PSC by irradiance equalization principle. The secondary objective is to extract the maximum power with negligible steady-state error. The accelerated linear convergence factor is employed to achieve irradiance equalization while minimizing the need to relocate modules, and it is accomplished within a reduced iteration count. The effectiveness of the proposed method is evaluated through simulation and experimental results. Various shading patterns are examined and compared against TCT_C /PO_M, $PSO_{R/M}$ and $CSHO_{R/M}$. The average output power enhancement of proposed $ALC\text{-}SHO_{R/M}$ method is 16.27% and 11.54% compared to TCT_R/PO_M and $PSO_{R/M}$ respectively. A performance analysis is carried out to provide additional insights into the efficacy of the proposed method.

References

[1] P. K. Ray, B. Subudhi, G. Putrus, M. Marzband, and Z. Ali, "Forecasting global solar insolation using the ensemble Kalman filter based clearness index model," in *CSEE Journal of Power and Energy Systems*, vol. 8, no. 4, pp. 1087–1096, Jul. 2022.

[2] K. T. Swetha and B. V. Reddy, "A novel constraint-based improved equilibrium optimization for global peak tracking of photovoltaic system under complex shading conditions," in *International Journal of Circuit Theory and Applications*, vol. 51, no. 6, pp. 2819–2838, 2023.

[3] O. Abdel-Rahim and H. Wang, "A new high gain DC-DC converter with model-predictive-control based MPPT technique for photovoltaic systems," in *CPSS Transactions on Power Electronics and Applications*, vol. 5, no. 2, pp. 191–200, Jun. 2020.

[4] T. Yang, X. Li, and S. Ding, "An improved constant power generation algorithm for photovoltaic systems," in *CPSS Transactions on Power Electronics and Applications*, vol. 7, no. 4, pp. 451–460, Dec. 2022.

[5] K. Rajani and T. Ramesh, "Reconfiguration of PV arrays (T-C-T, B-L, H-C) considering wiring resistance," in *CSEE Journal of Power and Energy Systems*, vol. 8, no. 5, pp. 1408–1416, Sept. 2022.

[6] B. Yang, H. Ye, J. Wang, J. Li, S. Wu, Y. Li, H. Shu, Y. Ren, and H. Ye, "PV arrays reconfiguration for partial shading mitigation: Recent advances, challenges and perspectives," in *Energy Conversion and Management*, vol. 247, p. 114738, 2021.

[7] P. R. Satpathy, P. Bhowmik, T. S. Babu, C. Sain, R. Sharma, and H. H. Alhelou, "Performance and reliability improvement of partially shaded PV arrays by one-time electrical reconfiguration," in *IEEE Access*, vol. 10, pp. 46911–46935, 2022.

[8] G. S. Krishna and T. Moger, "Improved Sudoku reconfiguration technique for total-cross-tied PV array to enhance maximum power under partial shading conditions," in *Renewable and Sustainable Energy Reviews*, vol. 109, pp. 333–348, 2019.

[9] S. Anjum and V. Mukherjee, "A novel arithmetic sequence pattern reconfiguration technique for line loss reduction of photovoltaic array under non-uniform irradiance," in *Journal of Cleaner Production*, vol. 331, p. 129822, 2022.

[10] G. Harish Kumar Varma, V. R. Barry, and R. K. Jain, "A novel magic square based physical reconfiguration for power enhancement in larger size photovoltaic array," in *IETE Journal of Research*, pp. 1–14, 2021.

[11] V. C. Chavan, S. Mikkili, and T. Senjyu, "Experimental validation of novel shade dispersion PV reconfiguration technique to enhance maximum power under PSCs," in *CPSS Transactions on Power Electronics and Applications*, vol. 8, no. 2, pp. 137–147, Jun. 2023.

[12] C. V. Chandrakant and S. Mikkili, "A typical review on static reconfiguration strategies in photovoltaic array under non-uniform shading conditions," in *CSEE Journal of Power and Energy Systems*, vol. 9, no. 6, pp. 2018–2039, Nov. 2023.

[13] H. K. V. Gadiraju, V. R. Barry, and R. K. Jain, "Improved performance of PV water pumping system using dynamic reconfiguration algorithm under partial shading conditions," in *CPSS Transactions on Power Electronics and Applications*, vol. 7, no. 2, pp. 206–215, Jun. 2022.

[14] F. Belhachat and C. Larbes, "PV array reconfiguration techniques for maximum power optimization under partial shading conditions: A review," in *Solar Energy*, vol. 230, pp. 558–582, 2021.

[15] X. Fang, Q. Yang, and W. Yan, "Switching matrix enabled optimal topology reconfiguration for maximizing power generation in series–parallel organized photovoltaic systems," in *IEEE Systems Journal*, vol. 16, no. 2, pp. 2765–2775, Jun. 2022.

[16] A. Fathy, "Butterfly optimization algorithm based methodology for

enhancing the shaded photovoltaic array extracted power via reconfiguration process," in *Energy Conversion and Management*, vol. 220, p. 113115, 2020.

[17] D. Yousri, T. S. Babu, S. Mirjalili, N. Rajasekar, and M. A. Elaziz, "A novel objective function with artificial ecosystem-based optimization for relieving the mismatching power loss of large-scale photovoltaic array," in *Energy Conversion and Management*, vol. 225, p. 113385, 2020.

[18] K. T. Swetha, B. V. Reddy, and R. K. Jain, "Dual-objective optimization for maximizing photovoltaic output power in a two-stage single-phase gridtied system," in *Energy Technology:Generation,Conversion,Storage,Distribution*, no. 2, p. 2300688, 2024.

[19] T. S. Babu, J. P. Ram, T. Dragičević, M. Miyatake, F. Blaabjerg, and N. Rajasekar, "Particle swarm optimization based solar PV array reconfiguration of the maximum power extraction under partial shading conditions," in *IEEE Transactions on Sustainable Energy*, vol. 9, no. 1, pp. 74–85, Jan. 2018.

[20] K. T. Swetha, V. R. Barry, A. Robinson, and R. K. Jain, "A novel spotted hyena optimization algorithm for MPPT under partial shading conditions," in *Proceedings of IECON 2021–47th Annual Conference of the IEEE Industrial Electronics Society*, 2021, pp. 1–6.

[21] G. Dhiman and V. Kumar, "Spotted hyena optimizer: a novel bioinspired based metaheuristic technique for engineering applications," in *Advances in Engineering Software*, vol. 114, pp. 48–70, 2017.

[22] E. R. Sanseverino, T. N. Ngoc, M. Cardinale, V. L. Vigni, D. Musso, P. Romano, and F. Viola, "Dynamic programming and munkres algorithm for optimal photovoltaic arrays reconfiguration," in *Solar Energy*, vol. 122, pp. 347–358, 2015.

Swetha K.T. was born in Kodagu, Karnataka. She received her B.Tech. degree in electrical and electronics engineering from the National Institute of Engineering-Institute of Technology, Mysuru, Karnataka, India in 2015, and the M.Tech. degree in power electronics and power systems from the National Institute of Technology Goa, Ponda, India, in 2017, where she is currently pursuing the Ph.D. degree with the Department of Electrical and Electronics Engineering. Her current research interests include renewable energy systems, PV array reconfigurations, multilevel inverters.

Barry Venugopal Reddy received his B.Tech. degree in electrical engineering from JNTU College of Engineering, Hyderabad, India in 2001, and the M.Tech. and Doctoral degrees from the National Institute of Technology, Warangal, India, in 2005 and 2013, respectively. He is currently working as an Associate Professor in the Department of Electrical Engineering, National Institute of Technology, Goa, India. His research interests include renewable energy systems, PV array reconfigurations, multilevel inverters, multilevel PWM switching strategies, multilevel inversion realized through open-end winding induction motor drives.